Hindawi
Journal of Nanomaterials
Volume 2022, Article ID 2137188, 7 pages
https://doi.org/10.1155/2022/2137188

Research Article

Solubilization and In Vitro Physical and Chemical Properties of the Amorphous Spray-Dried Lactose-Luteolin System

Liping Dong[1,2] **Bo Wang**[1] **Lin Chen**[1] **and Min Luo**[3,4]

[1]*Xiangya School of Pharmaceutical Sciences, Central South University, Changsha 410013, China*
[2]*Academician Workstation, Changsha Medical University, Changsha 410219, China*
[3]*Department of Nephrology, The Second Xiangya Hospital, Central South University, Changsha, 410011 Hunan Province, China*
[4]*Department of Rehabilitation Medicine and Health Care, Hunan University of Medicine, Huaihua, 418000 Hunan Province, China*

Correspondence should be addressed to Bo Wang; 197211030@csu.edu.cn and Min Luo; xyluomin@csu.edu.cn

Received 21 February 2022; Revised 11 March 2022; Accepted 14 March 2022; Published 12 April 2022

Academic Editor: Weiguo Li

Luteolin is a hydrophobic drug with low solubility, which has many limitations in practical use. To improve solubility, a spray drying technique was used to prepare complexes with lactose to promote the solubility and bioavailability of luteolin. The solution samples were spray dried using different ratios of water and ethanol as different dissolution media. By characterizing the spray-dried powders obtained, we found that the solubility of the different groups of samples obtained by spray drying was improved, and similarly, their dissolution rates were also increased to different degrees. By comparison, both luteolin and the cofactor lactose were able to achieve high dissolution rates at suitable solution ratios and formed amorphous eutectic crystals after the spray drying process, which contributed well to the increased solubility and altered dissolution efficiency of luteolin.

1. Introduction

Many food-derived phytochemicals and their derivatives, such as curcumin, resveratrol, and luteolin, have great potential in the treatment of cancer. Luteolin (3,4,5,7-tetrahydroxyflavones) is a common phytochemical flavonoid found in a variety of plants such as celery chrysanthemums, bell peppers, carrots, onion leaves, and broccoli and has a variety of biological effects such as anti-inflammatory, antiallergic, and anticancer [1, 2]. Various lignan-rich plants have long been used in traditional Chinese, Iranian, and Brazilian medicine to treat many diseases such as inflammation, cardiovascular disease, and cancer. Their pharmacologically active anti-inflammatory effects may be related to their anticancer properties [3].

Inflammation is a complex biochemical response in which immune and nonimmune cells are highly coordinated. Inflammation is a natural response to harmful stimuli, such as tissue stress, injury, and microbial invasion, in order to maintain a state of homeostasis in the body [4–6]. The main aim of the inflammatory response is to eliminate harmful stimuli, and during the inflammatory response, immune cells secrete several types of mediators, including cytokines (e.g., interferon-like, interleukin, and tumor necrosis factor-α) and chemokines (e.g., monocyte chemotactic protein 1), produced tumor necrosis factor-alpha interferon beta and granulocyte-macrophage colony-stimulating factor (all proinflammatory cytokines), and increased levels of IL-10 [7–9]. Luteolin exerts their effects by altering these signaling pathways (including nuclear factor-κB) [10–12]. Cancer is a large group of diseases characterized by evasion of apoptosis, unlimited replicative potential, ongoing angiogenesis, tissue invasion and metastasis, and evasion of immune surveillance [13]. Luteolin is known to inhibit kinases, regulate the cell cycle, induce apoptosis, and reduce transcription factors through various mechanisms. The anticancer properties of luteolin are associated with the induction of apoptosis, which involves redox regulation, deoxyribonucleic acid damage, and inhibition of cancer cell proliferation by protein kinases, as well as

inhibition of metastasis and angiogenesis. In addition, luteolins can sensitize various cancer cells to treatment-induced cytotoxicity by inhibiting cell survival pathways and stimulating apoptotic pathways, while luteolin acts by altering a number of signaling pathways and exerts inhibitory and therapeutic effects on cancers such as breast, colon, pancreatic, prostate, and oral cancers through a variety of mechanisms [1, 10, 14–16].

However, luteolin is a refractory bioactive compound, and its inherent low water solubility (1.93×10^{-5} mol/l) and low oral bioavailability hinder its clinical application. Therefore, the aim of this study was to prepare and study various solid dispersions of luteolin by high solubility in ethanol in order to improve its solubility and bioactivity [17–20]. Spray drying technology is one of the best ways to prepare solid dispersions because of its proven technology and ease of operation [21]. The commonly used excipient lactose is used as a carrier, and different solvents are used as dispersion media. In the preparation process, lactose was codispersed with luteolins in the dispersion medium and prepared in the same spray drying condition. The powder samples obtained were characterized by differential scanning calorimetry (DSC), X-ray diffraction (XRD), and scanning electron microscopy (SEM), and the in vitro solubility and powder properties of luteolin were evaluated.

2. Materials and Methods

2.1. Chemical Materials. Luteolin (≥98.0%) was purchased from Xi'an Ruidi-Bio Technology Co., Ltd. Lactose (≥99.9%) was accessed from Dawning Pharmaceutical Co., Ltd., China. Absolute ethanol (purity ≥ 99.7%) for luteolin dissolution was purchased from Shanghai Titan Technology Co., Ltd.; the purified water was made from our own laboratory in fresh. All the chemical materials used in this experiment are of analytical/pharmaceutical grade with high purity.

2.2. Preparation of Physical Mixture. The lactose crystals were accurately weighed with luteolin, and the pharmaceutical grade lactose and luteolins were mixed at a mass ratio of 9 : 1 using the physical mixing method to obtain a homogeneous mixture. The physical mixture obtained was properly sieved using a no. 60 sieve to remove potentially larger particles and stored in a desiccator pending further characterization.

2.3. Preparation of Sample Solutions/Suspensions. Lactose crystals and luteolin were accurately weighed and then sieved separately to avoid potential slow dissolution problems and then kept separately in a desiccator for backup. Suspension A was prepared using pure water by first dissolving 9.0 g of pharmaceutical grade lactose in water and adding 1.0 g of luteolin under stirring to obtain suspension A, which was then stirred continuously under sealed conditions.

Lactose and luteolin were weighed separately according to the same method, and then, lactose and luteolin were dissolved in different solvents, where lactose was dissolved in pure water and luteolin in anhydrous ethanol. Both solutions were sonicated simultaneously at 40.0 kHz for 10.0 minutes, and after the two components were completely dissolved, the ethanol solution of luteolin was slowly poured into the aqueous solution of lactose along a glass rod and stirred thoroughly at low speed (30.0 rpm/min) to mix well while avoiding crystallization of the two substances as much as possible to obtain solution B.

2.4. Setting of Spray Dryer Parameters. The experimental process was carried out using a small spray dryer BYC-015. The spray drying process was protected by a nitrogen flow rate of 28.0 kg/h to prevent the organic phase ethanol from exploding in contact with oxygen in a high-temperature environment. The solution flow rate was 15.0 ml/min and was carried out using a nozzle with a diameter of 1.0 mm. The two solutions were sprayed separately under identical conditions and completed continuously. The parameters of the spray drying process were kept constant during the spray drying process: fan frequency 50.0 ± 0.5 Hz, inlet gas temperature 140.0 ± 1.0°C, outlet gas temperature 130.0 ± 3.0°C, and spray pressure 0.20 ± 0.01 MPa. After the spraying process, each sample was obtained separately in the collection hopper, sealed, and stored, respectively.

2.5. Characterization of Samples

2.5.1. Solubilization Experiments. In order to investigate the solubilizing effect of the spray drying process on luteolin and the effect on its dissolution state, a physical mixture of luteolin and the excipient lactose was prepared according to the formulation, and two spray-dried samples A and B were pressed into tablets at the same pressure, 0.30 g each, and prepared in triplicate to obtain disintegration solubility data. Dissolution data were obtained from an RC1210G Dissolution Analyzer (Xinzhi, China) with a paddle method of extraction at 75.0 rpm/min, 37.0 ± 0.1°C, and a sampling height of 750.0 ml. During the dissolution process, 1.0 ml of each sample was taken at different time intervals using a sampling needle and the standard solution was replenished promptly until the dissolution process was completed.

2.5.2. Ultraviolet-Visible Spectrophotometer (UV-Vis). The solution obtained from the dissolution experiment was filtered through a microporous membrane and diluted in the same multiples to configure the required test sample. The diluted solutions were poured individually into quartz dishes, the absorbance was measured using a UV-Vis spectrophotometer, and the solubility curve was plotted against the absorbance. The instrument used for this experiment was a UV-2401pc spectrophotometer (Shimadzu, Kyoto, Japan).

2.5.3. Differential Scanning Calorimetry (DSC). To check the physical crystalline state of the samples, thermodynamic analyses of lactose, xylitol, physical mixtures, and spray-dried samples were carried out using a differential scanning calorimeter (HSC-4 DSC, Henven, China). Samples for DSC determination were prepared in sealed, crimped aluminum pans according to standard procedures. Approximately 9.5 ± 0.3 mg of each specimen was used for analysis at a temperature range of 35.0-400.0°C and a slope of 5.0°C/min.

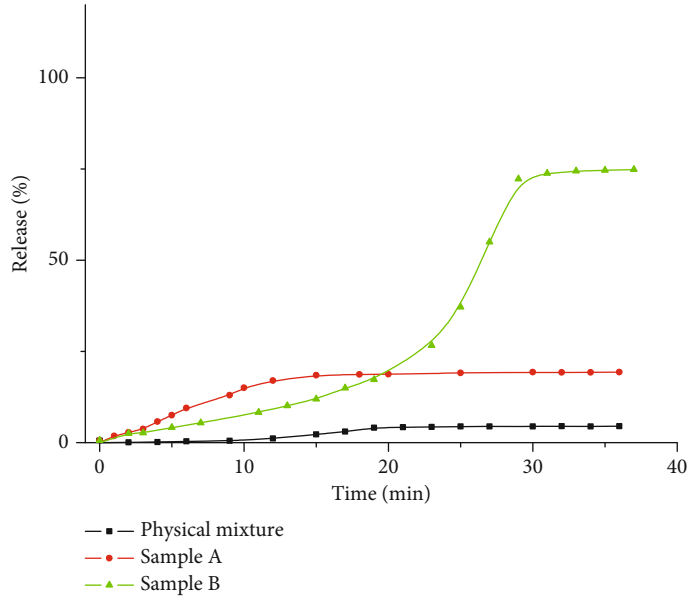

Figure 1: Release spectra of luteolin tablets in two samples and physical mixture of the same formulation.

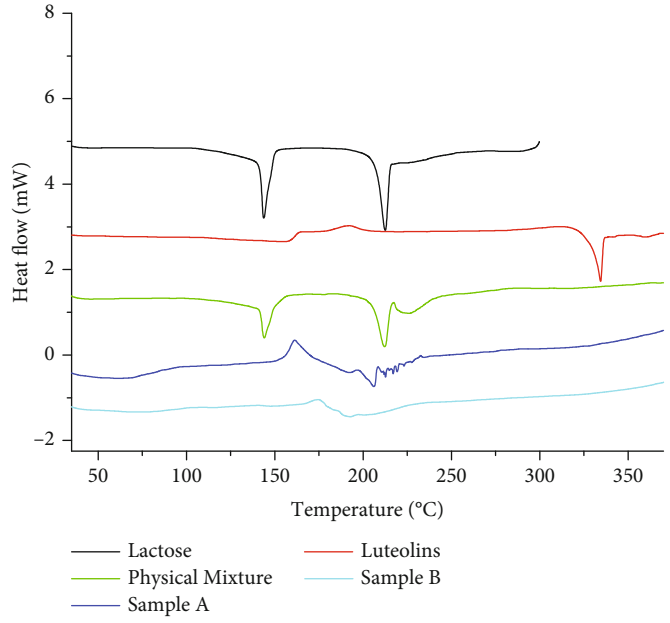

Figure 2: DSC plots of raw materials, physical mixtures of the same formulation, and samples from the experiments.

2.5.4. Thermogravimetric Analyzer (TGA). Samples were analyzed using a thermogravimetric analyzer (TGA Q5000 V3.17 Build 265). N_2 was used as the equilibrium gas during this process. The temperature during thermogravimetric analysis is 35.0-400.0°C, and the heating rate is 5.0°C/min. Samples are also examined in an alumina pan.

2.5.5. Scanning Electron Microscopy (SEM). In order to observe the surface morphology of the specimen powders, the specimen powders were uniformly plated with gold and subsequently placed on aluminum specimen stakes with carbon strips. The gold-plated specimens were examined using a JSM-7200F Scanning Electron Microscope (SEM, JEOL Ltd.).

2.5.6. N_2 Adsorption. Separate mesoporous adsorption experiments were carried out on powder samples to assess the differences in pore size distribution, surface area, and pore volume of different samples to determine the effect of different dissolution states of solutes in different spray feedstocks on their powder state.

2.5.7. X-Ray Diffraction (XRD). XRD analysis is used to study the crystalline behavior of samples. Solid samples were mounted on a powder holder, and samples were analyzed using

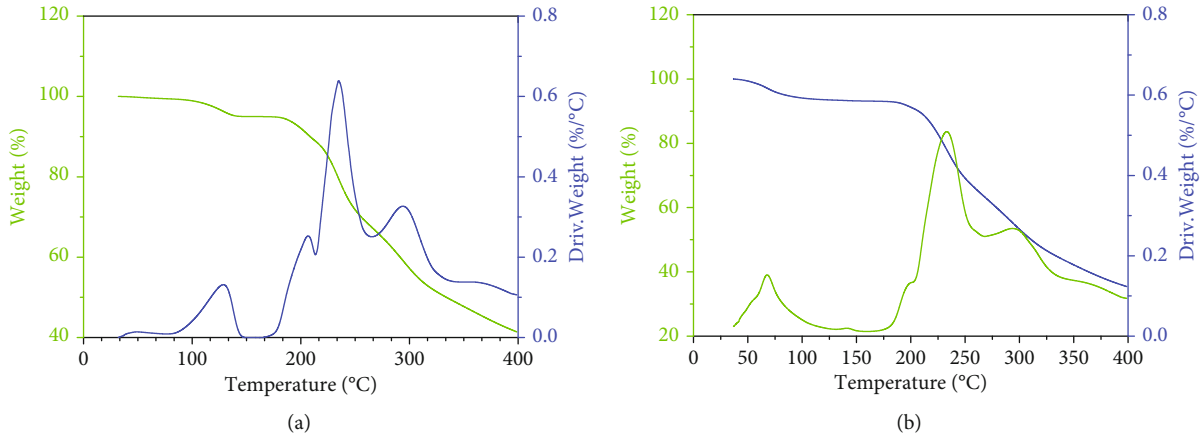

Figure 3: TGA curves of two spray-dried samples from the experiment: sample A (a) and sample B (b).

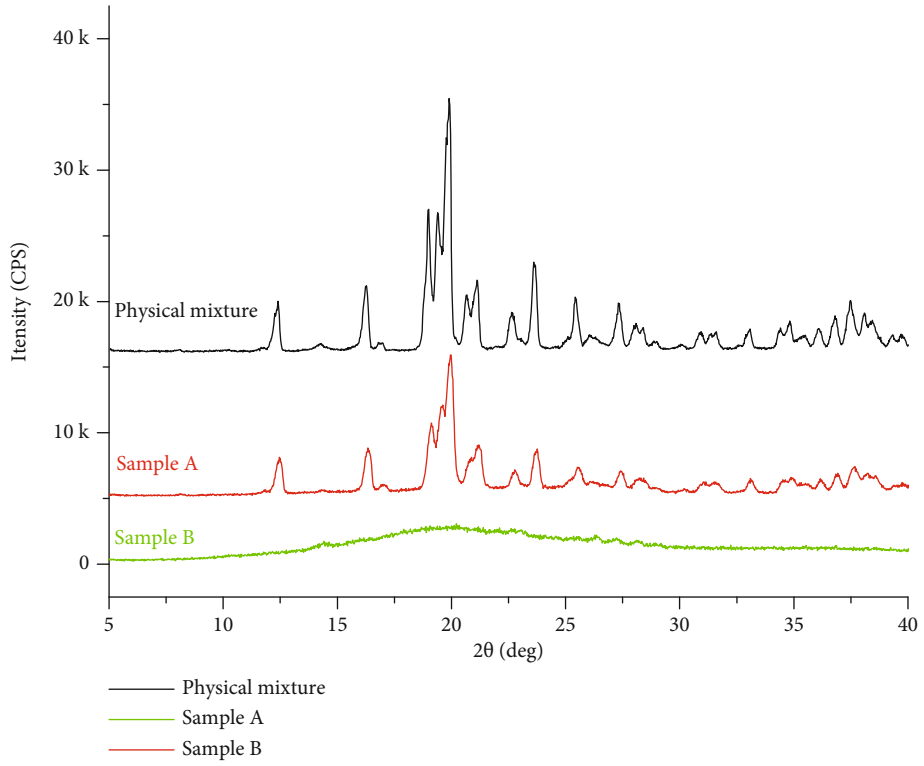

Figure 4: XRD curves of the physical mixture of the same formulation and of the two spray-dried samples from the experiment.

a Siemens D5000 diffractometer with a scan rate of 0.02°/s, a scan current of 30.0 mA, and a scan voltage of 40.0 kV.

3. Results and Discussion

Dissolution curves were plotted based on the absorbance of the sample solutions obtained by sampling at different stages of the dissolution process, as shown in Figure 1. For the physical mixture, luteolin was less water soluble and less than 5.0% of the drug was released during this dissolution process. In contrast, the release rate of both sample powders increased significantly after the complete disintegration of the drug following the spray drying process. Sample B showed a significant increase in release rate. Comparing sample A and sample B, we found that the percentage release was significantly higher for sample B, but the dissolution rate was relatively smaller than that of sample A, and it took more time to reach dissolution equilibrium. It is possible that this is due to the fact that a higher proportion of ethanol in the same solution makes luteolin more soluble, resulting in the analytical release of more luteolin molecules from the lattice and destroying the crystalline structure of luteolin during the spray drying process, resulting in more amorphous luteolin being formed, leading to a significant increase in its solubility. Similarly, in this process, due to the lower solubility of lactose in ethanol, more lactose crystals

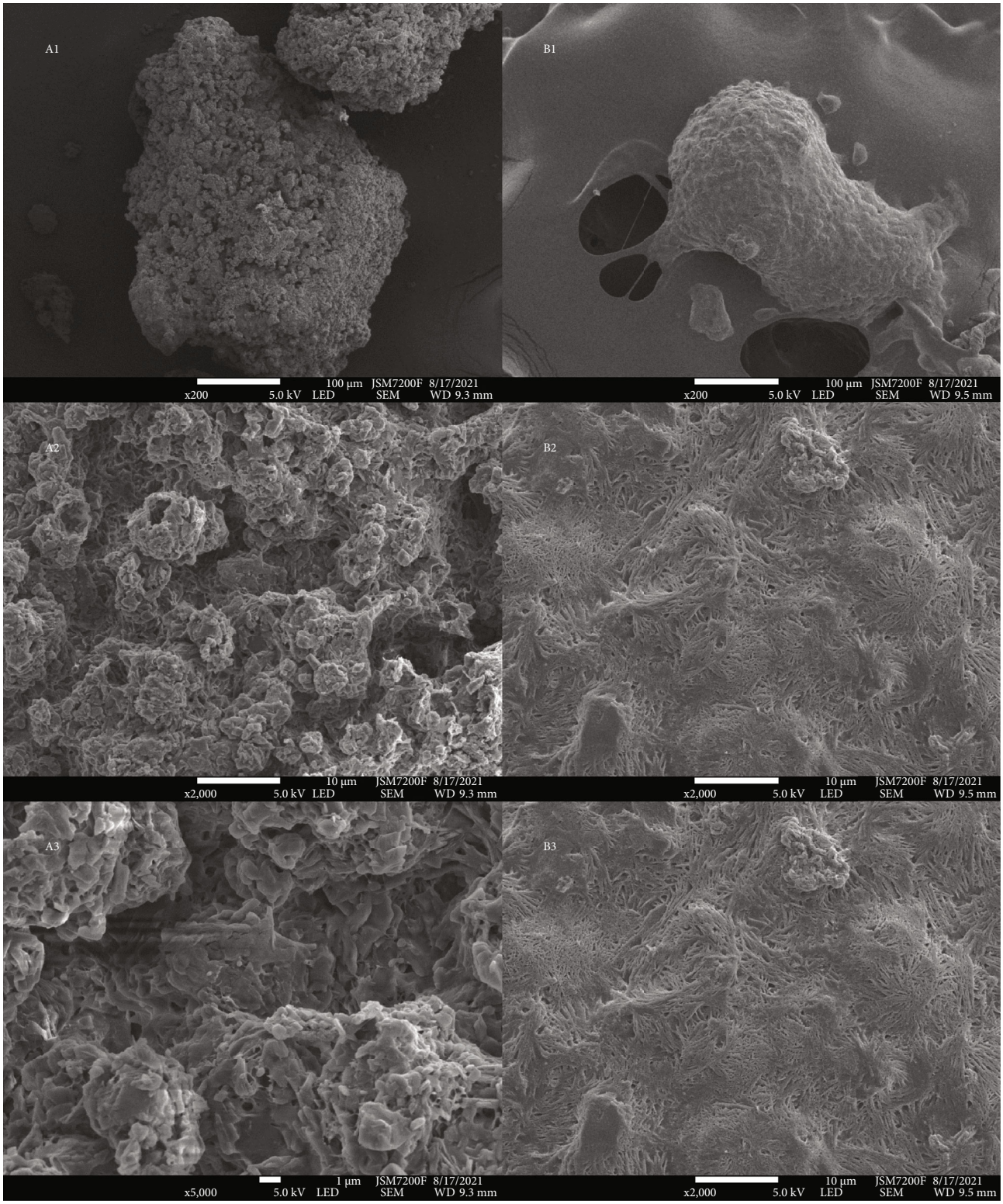

Figure 5: SEM images of spray-dried samples obtained in two experiments at 200x, 2000x, and 5000x (A1-3 for sample A; B1-3 for sample B).

precipitated prior to the high-temperature drying process, the proportion of amorphous lactose was reduced, and the crystalline form of the powder in the tablets pressed from the sample B powder was more complex, making the overall system more difficult to disintegrate.

We carried out thermal analysis of the constituent materials in the experiment. By analyzing the DSC curves of the samples (Figure 2), the water of crystallization and heat absorption peaks of lactose monohydrate and the melting peak of lactose crystals occurred at 144.3°C and 213.4°C,

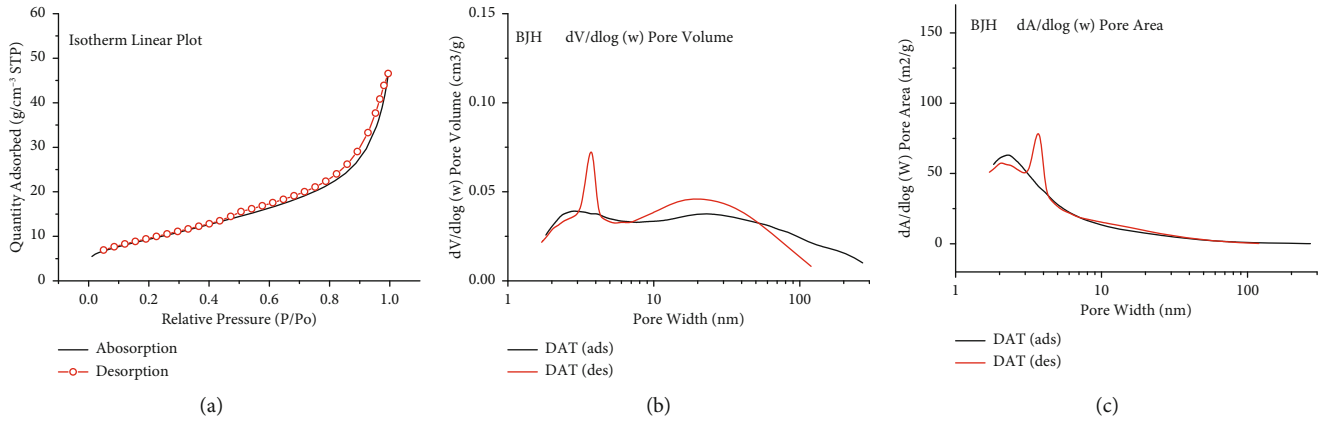

Figure 6: Nitrogen adsorption curves for sample B obtained from the experiments: isotherm linear plot (a), BJH adsorption/desorption $dV/d\log(w)$ pore volume (b); BJH adsorption/desorption $dA/d\log(w)$ pore (c).

respectively, while the maximum heat absorption peak of xylitol occurred at 334.4°C. For the physical mixture, the heat absorption peak of lactose shifted towards the lower-temperature region with the maximum heat absorption occurring at 212.1°C, while the heat absorption peak of xylitol disappeared near 334.0°C and a broad and blunt heat absorption peak appeared near the lactose heat absorption peak with its peak shifted to 226.1°C, which may be related to the slower heat transfer rate of the solid mixture. In contrast, for the spray-dried sample, the overall peak pattern changed dramatically, with the disappearance of the crystalline water peak for lactose, a reduction in the crystalline melting peak for lactose and luteolin, and an upward exothermic peak acting towards the lower temperature region, indicating the possible appearance of an amorphous product. By comparing sample A and sample B, the amorphous exothermic peak of sample A appeared at 160.8°C with a larger heat absorption peak at 205.8°C. In addition, a complex and fine heat absorption peak appears during sustained heating, which may be due to differences in the enthalpy of melting due to polycrystal formation, suggesting that a more complex crystal composition may be present. In contrast, for sample B, the exothermic peak shifted towards the high-temperature region, reaching 175.5°C. During heating, no small peaks similar to those of sample A appear and the heat flow curve is flat throughout. This indicates that in sample B, the crystalline form is relatively homogeneous and a relatively pure amorphous product, suggesting that both luteolin and lactose are well soluble in the appropriate proportions of ethanol solution and that both can exist as free molecules in spray drying under high-temperature conditions, rapidly losing water to form an amorphous product.

Figure 3 shows the thermogravimetric curves of these two groups of samples in order from left to right. These two sets of samples show the same trend of weight loss with increasing temperature. These samples show a trend of weight loss after 50.0°C, reaching a maximum rate at around 260.0°C. A comprehensive analysis of these two sets of samples showed that the physical composition of the spray-dried powders obtained from the different concentrations of solutions was essentially the same, but the proportions of crystalline components showed significant differences and the weight loss trends were approximately the same for both sets of samples; however, there were differences in the weight loss curves at around 200.0°C; samples A and B may have different crystalline compositions.

According to the XRD curves (Figure 4), the α-lactose peaks at 2θ were 12.5°, 19.1°, 19.6°, and 19.9° in the two samples, respectively, while the β-lactose peak at $2\theta = 10.5°$ was absent in both samples, indicating that no lactose swirling occurred during the dissolution and spray drying process or it occurred in a very small proportion. The diffraction pattern showed that the individual diffraction peaks in the physical mixture were sharp and steep and that the individual diffraction peaks in sample A became relatively short and flat compared to the physical mixture, indicating a possible reduction in crystalline material, while the diffraction peaks at different positions in sample B disappeared and were replaced by a large blunt and flat amorphous peak at around $2\theta = 20.0°$. This suggests that the proportion of crystalline material in the sample was reduced during the spray drying process, particularly in sample B, where the whole composition was able to transform into an amorphous state after dissolution in a suitable solution and after the spray drying process.

tBased on electron microscopic observations, sample A and sample B exhibited completely different states in the SEM field of view (Figure 5). Sample A exhibits a porous aggregate of various fine crystal particles with relatively smooth solid bridges wrapped between the crystal particles, indicating the presence of some amorphous components in the powder of sample A. During the spray drying process, the undissolved solid components in solution were dried together with the solution, and the dissolved molecules in solution partially crystallized and partially wrapped around the surface of the crystals in an amorphous state, forming a rough aggregate of solid particles. On the other hand, sample B shows a different crystalline/noncrystalline state. Unlike sample A, the surface of sample B is very smooth and porous with no apparent granular structure, indicating that most of the components in sample A are probably in a noncrystalline state.

For sample B, which was in a porous state, nitrogen adsorption experiments were carried out to calculate and evaluate its pore structure (Figure 6). Its BET adsorption and

desorption curves visually represent its porosity. Its average pore size was calculated by analysis to be approximately 7.4 nm, with a cumulative volume of pores with widths between 1.7000 nm and 300.0000 nm: 0.069187 cm^3/g. The BET surface area (33.8243 m^2/g), whose large pore volume may provide better compressibility, confirms the trend of the solubility curve.

4. Conclusion

To improve the solubility of luteolin, a complex with lactose was prepared by the spray drying technique to promote the solubility and bioavailability of luteolin. The experimental results showed that the solubility and dissolution efficiency of the spray-dried drug were significantly higher compared to those of the solid mixture. The spray drying resulted in a higher proportion of amorphous products in the drug product powder. The amorphous content of the product could be significantly altered by changing the ratio of the components in the dissolution medium to form a porous eutectic product with a smooth surface, which could contribute to the enhancement of the solubility of luteolin and its clinical application.

Data Availability

All data used to support the findings of this study are included within the article.

Disclosure

Liping Dong is a postdoctor under the supervision of Professor Wenhu Zhou in Xiangya School of Pharmaceutical Sciences, Central South University.

Conflicts of Interest

There is no conflict of interest regarding the publication of this paper.

Acknowledgments

The work is supported by the Postdoctoral Start-up Fund from Central South University. This work is also supported by the Foundation of the Second Xiangya Hospital (XYEYY20200812).

References

[1] Y. Lin, R. Shi, X. Wang, and H. M. Shen, "Luteolin, a flavonoid with potential for cancer prevention and therapy," *Current Cancer Drug Targets*, vol. 8, no. 7, pp. 634–646, 2008.

[2] S. F. Nabavi, N. Braidy, O. Gortzi et al., "Luteolin as an anti-inflammatory and neuroprotective agent: a brief review," *Brain Research Bulletin*, vol. 119, Part A, pp. 1–11, 2015.

[3] N. Aziz, M. Y. Kim, and J. Y. Cho, "Anti-inflammatory effects of luteolin: a review of in vitro, in vivo, and in silico studies," *Journal of Ethnopharmacology*, vol. 225, pp. 342–358, 2018.

[4] K. Roe, "An inflammation classification system using cytokine parameters," *Scandinavian Journal of Immunology*, vol. 93, no. 2, article e12970, 2021.

[5] N. Singh, D. Baby, J. P. Rajguru, P. B. Patil, S. S. Thakkannavar, and V. B. Pujari, "Inflammation and cancer," *Annals of African Medicine*, vol. 18, no. 3, pp. 121–126, 2019.

[6] R. Medzhitov, "Origin and physiological roles of inflammation," *Nature*, vol. 454, no. 7203, pp. 428–435, 2008.

[7] J. Iype and M. Fux, "Basophils orchestrating eosinophils' chemotaxis and function in allergic inflammation," *Cell*, vol. 10, no. 4, p. 895, 2021.

[8] A. Sgambato and A. Cittadini, "Inflammation and cancer: a multifaceted link," *European Review for Medical and Pharmacological Sciences*, vol. 14, no. 4, pp. 263–268, 2010.

[9] D. Wallach, T. B. Kang, and A. Kovalenko, "Concepts of tissue injury and cell death in inflammation: a historical perspective," *Nature Reviews. Immunology*, vol. 14, no. 1, pp. 51–59, 2014.

[10] M. Imran, A. Rauf, T. Abu-Izneid et al., "Luteolin, a flavonoid, as an anticancer agent: a review," *Biomedicine & Pharmacotherapy*, vol. 112, 2019.

[11] F. Ali and Y. H. Siddique, "Bioavailability and pharmacotherapeutic potential of luteolin in overcoming Alzheimer's disease," *CNS & Neurological Disorders Drug Targets*, vol. 18, no. 5, pp. 352–365, 2019.

[12] W. C. Huang, C. J. Liou, S. C. Shen, S. Hu, C. Y. Hsiao, and S. J. Wu, "Luteolin attenuates IL-1β-induced THP-1 adhesion to ARPE-19 cells via suppression of NF-κB and MAPK pathways," *Mediators of Inflammation*, vol. 2020, Article ID 9421340, 15 pages, 2020.

[13] G. Kroemer and J. Pouyssegur, "Tumor cell metabolism: cancer's Achilles' heel," *Cancer Cell*, vol. 13, no. 6, pp. 472–482, 2008.

[14] C. J. Wruck, M. Claussen, G. Fuhrmann et al., "Luteolin protects rat PC12 and C6 cells against MPP+ induced toxicity via an ERK dependent Keapl-Nrf2-ARE pathway," *Journal of Neural Transmission. Supplementum*, vol. 72, pp. 57–67, 2007.

[15] S. Ahmed, H. Khan, D. Fratantonio et al., "Apoptosis induced by luteolin in breast cancer: mechanistic and therapeutic perspectives," *Phytomedicine*, vol. 59, 2019.

[16] R. K. Ambasta, R. Gupta, D. Kumar, S. Bhattacharya, A. Sarkar, and P. Kumar, "Can luteolin be a therapeutic molecule for both colon cancer and diabetes?," *Briefings in Functional Genomics*, vol. 18, no. 4, pp. 230–239, 2018.

[17] S. Alshehri, S. S. Imam, M. A. Altamimi et al., "Enhanced dissolution of luteolin by solid dispersion prepared by different methods: physicochemical characterization and antioxidant activity," *ACS Omega*, vol. 5, no. 12, pp. 6461–6471, 2020.

[18] G. Wu, J. Li, J. Yue, S. Zhang, and K. Yunusi, "Liposome encapsulated luteolin showed enhanced antitumor efficacy to colorectal carcinoma," *Molecular Medicine Reports*, vol. 17, no. 2, pp. 2456–2464, 2018.

[19] M. Mahin, A. Ali, K. Elahe et al., "Synthesis of a copolymer carrier for anticancer drug luteolin for targeting human breast cancer cells," *Journal of Traditional Chinese Medicine*, vol. 39, no. 4, pp. 474–481, 2019.

[20] M. Imran, R. Mehmood, U. R. Mughal, B. Ali, and A. Malik, "Vicarin, a new isoflavone from Eremostachys vicaryi," *Journal of Asian Natural Products Research*, vol. 14, no. 3, pp. 293–296, 2012.

[21] B. Wang, F. Liu, J. Xiang et al., "A critical review of spray-dried amorphous pharmaceuticals: synthesis, analysis and application," *International Journal of Pharmaceutics*, vol. 594, 2021.